Available online at www.sciencedirect.com
ScienceDirect
Bioorganic & Medicinal Chemistry 15 (2007) 1659–1669
Bioorganic & Medicinal Chemistry

Biological profile of new apoptotic agents based on 2,4-pyrido[2,3-*d*]pyrimidine derivatives

Lucía Cordeu,[a,*] Elena Cubedo,[a] Eva Bandrés,[a] Amaia Rebollo,[a] Xabi Sáenz,[b] Hector Chozas,[b] M[a] Victoria Domínguez,[b] Mikel Echeverría,[b] Beatriz Mendivil,[b] Carmen Sanmartin,[b] Juan Antonio Palop,[b] María Font[c] and Jesús García-Foncillas[a]

[a]*Laboratorio de Farmacogenómica, Área de Oncología, Centro de Investigación Médica Aplicada, Pamplona, Spain*
[b]*Sección de Síntesis, Departamento de Química Orgánica y Farmacéutica, Universidad de Navarra, Pamplona, Spain*
[c]*Sección de Modelización Molecular Departamento de Química Orgánica y Farmacéutica, Universidad de Navarra, Pamplona, Spain*

Received 9 October 2006; revised 23 November 2006; accepted 8 December 2006
Available online 12 December 2006

Abstract—In order to obtain less toxic antitumoral compounds we have looked for novel compounds with anticancer activity based on proapoptotic mechanisms. The compounds studied in this work are derivatives of bicyclic aromatic systems like pyrido[2,3-*d*]pyrimidines. The potential antitumoral activity of the compounds was evaluated in vitro by examining their cytotoxic effects against human breast, colon, and bladder cancer lines (MD-MBA-231, HT-29, and T-24). The data indicate that HC-6 is a potent anticancer drug showing dose-dependent cytostatic and proapoptotic effects through activation of two different signaling pathways namely a pathway leading to cell cycle arrest and a transcription-independent route leading to rapid apoptosis.

1. Introduction

The understanding of the molecular mechanisms involved in cancer has opened new ways in the development of new anticancer compounds. It is now accepted that tumor growth depends on a balance between an enhanced proliferation and reduced rates of cell death. We have gained remarkable biological knowledge about the exact steps necessary for cancer cells to grow, divide, and spread. This has opened the door for new prospects in chemotherapy to stop or reverse this proliferative process, especially using targeted approaches based on regulation of the cancer cell cycle and regulation of apoptotic pathways.[1]

Apoptosis is a physiological process for killing cells and is critical for the normal development and function of multicellular organism. Abnormalities in cell death control can contribute to a variety of diseases, including cancer.[2–4] Signaling for apoptosis occurs through multiple independent pathways that are initiated either by triggering events within the cell or from outside the cell. All apoptosis signaling pathways converge on a common machinery of cell destruction that is mainly activated by a family of cysteine proteases called caspases that cleave proteins at aspartate residues.[5–7] Dismantling and removal of apoptotic cells is accomplished by proteolysis of vital cellular constituents, DNA degradation, and phagocytosis by neighboring cells.[4]

In the search of less toxic anticancer therapies, we have looked for novel compounds with anticancer activity based on a proapoptotic mechanism. Drugs that restore the normal apoptotic pathways have the potential for effectively treating cancers that depend on aberrations of the apoptotic pathway to stay alive, and many apoptosis targets are currently being explored for cancer drug discovery.[1,8,9] A number of nucleoside analogues have been either used clinically as anticancer drugs or evaluated in clinical studies, while new nucleoside analogues continue to show promise.[10] In this article, we report the biological activities of a series of new pyrido[2,3-*d*]pyrimidine nucleosides to explore the possibility of these compounds as potential anticancer drugs. This family of compounds have been demonstrated to specifically inhibit tyrosine kinases.[11–16] Protein tyrosine kinases have been characterized as participating in a

Abbreviations: DMSO, dimethylsulfoxide; PMSF, phenyl-methyl-sulfonyl fluoride; DTT, Dithiothreitol.
Keywords: Apoptosis induction; Pyridopyrimidine derivatives.
* Corresponding author. Tel.: +34 948 194700x1023; fax: + 34 948194714; e-mail: lcorver@alumni.unav.es

0968-0896/$ - see front matter © 2006 Elsevier Ltd. All rights reserved.
doi:10.1016/j.bmc.2006.12.010

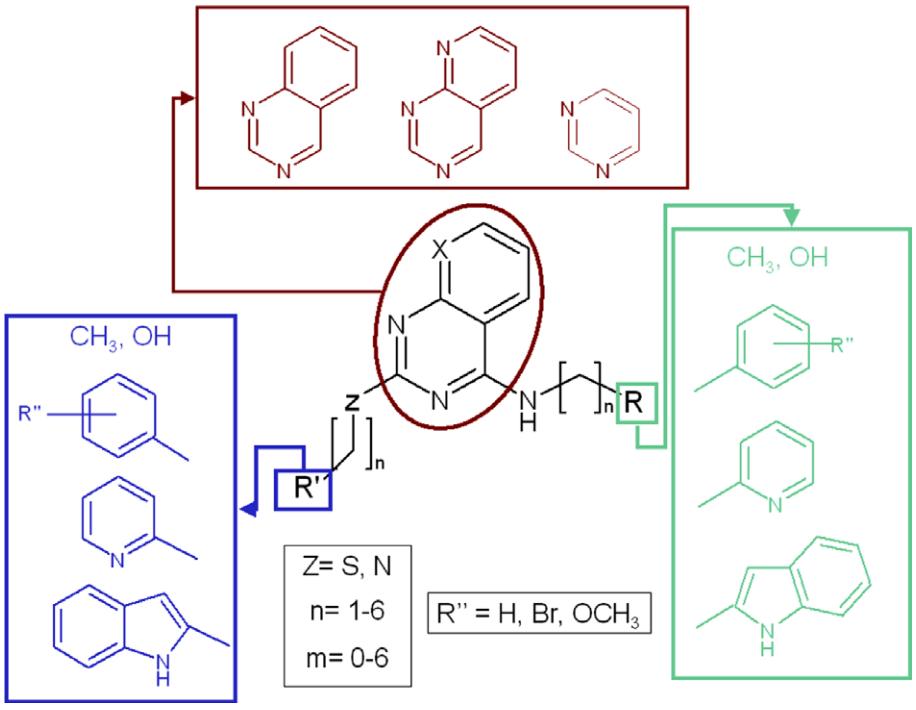

Figure 1. General diagram of the molecules included in this work.

number of cellular signaling events including mitogenesis processes. Many tyrosine kinases have been shown to be increased in either expression or activity in a large percentage of tumor types and increased tyrosine phosphorylation has been associated with progression of disease and poor prognosis.[17–19]

In the structural design for this study, a general pattern derived from the reference literature has been adopted. This pattern, while flexible in geometry and chemical structure has a central nucleus made up of an aromatic system, the ring of pyrido[2,3-*d*]pyrimidine, connected to two identical lateral arms consisting of an amine aliphatic chain of variable length and flexibility with or without heterocycles at the end of the chain (Fig. 1). This paper is a continuation of our previous work in the field of cytotoxicity and apoptosis. Recently, we have described the synthesis of symmetrical and asymmetrical derivatives as cytotoxic and apoptosis inducers.[20–23]

In the present study, we investigated the antitumoral action of a series of 20 pyridopyrimidines. We found that HC-6 shows a good profile as an apoptosis inducer, activating caspase-3 and inducing DNA fragmentation at a micromolar range in several cancer cell lines. These findings indicate that HC-6 is a promising candidate as a novel therapeutic agent.

2. Results

2.1. Cytotoxicity

The cytotoxic activities of the synthesized compounds were determined in three tumoral cell lines, breast (MD-MBA-231), bladder (T-24), and colon (HT-29), using the neutral red assay at the screening concentrations of 100 and 20 μM. We used camptothecin as reference substrate. Its IC_{50} values were 0.291 μM in MD-MB-231, 0.014 μM in HT-29, and 0.006 μM in T-24. All compounds developed toxic activity in some of the three cell lines tested. The IC_{50} values are shown in Table 1. In general, we observed that compounds had a more potent effect against the breast cancer cell line.

2.2. Apoptosis detection: caspase-3 activity and DNA fragmentation

Once we tested the cytotoxic action of the compounds we wanted to discern if this fact was due to an apoptotic or a necrotic stimulus. The presence of oligonucleosomal fragments in the cell cytoplasm is a consequence of DNA fragmentation and is considered a hallmark of apoptosis. The ability of the selected compounds to induce DNA fragmentation was assessed using the Cell Death Detection ELISA Plus Kit (Roche) after 24 h of incubation with the compounds. The level of DNA degradation measured in the control culture was considered as 1. The results are shown as enrichment factor (EF) expressing the number of times in which the culture containing the test compounds surpasses the control culture in its ability to induce DNA fragmentation. The results obtained for the compounds are shown in Figure 2.

The compounds were also subjected to a caspase-3 activation assay because this enzyme is considered to be one of the principal executing caspases involved in the development of the apoptotic program. The levels of this enzyme were measured at 14, 24, and 48 h using flow

Table 1. IC_{50} values and goodness of curve fitting (r^2) of the compounds in three human tumor cell lines

Compound	IC_{50} (μM)					
	HT-29	r^2	T-24	r^2	HTB-26	r^2
VD-3	24.1	0.88	21.5	0.71	1.3	0.75
VD-4	22.5	0.85	5.9	0.88	1.4	0.88
VD-5	19.9	0.88	5.3	0.87	2.6	0.71
VD-8	20.2	0.89	15.8	0.88	9.5	0.78
VD-9	24.4	0.64	8	0.77	7	0.65
VD-11	25.2	0.79	7.9	0.78	5.6	0.65
VD-14	0.6	0.86	0.7	0.64	1.2	0.79
VD-22	4.2	0.99	4.6	0.81	2.1	0.99
VD-27	18.4	0.87	18.5	0.90	9	0.86
VD-29	3.6	0.79	10.6	0.65	8.4	0.83
XS-1	2.5	0.93	8.1	0.98	1.2	1.00
XS-2	1.7	0.94	13.2	0.97	5.8	0.90
XS-3	5	0.72	1.4	0.87	1.1	0.87
XS-4	4.2	0.97	11.5	0.84	2.7	0.75
ME-43	67.6	0.98	NT	NT	NT	NT
ME-44	3	0.79	7.7	0.97	5.1	0.76
HC-1	11	0.76	13.4	0.98	10.3	0.87
HC-2	7.5	0.72	5	0.97	3.2	0.78
HC-3	15	0.80	11	0.67	8.3	0.94
HC-6	8.9	0.90	5	0.87	1.5	0.79

NT, not toxic.

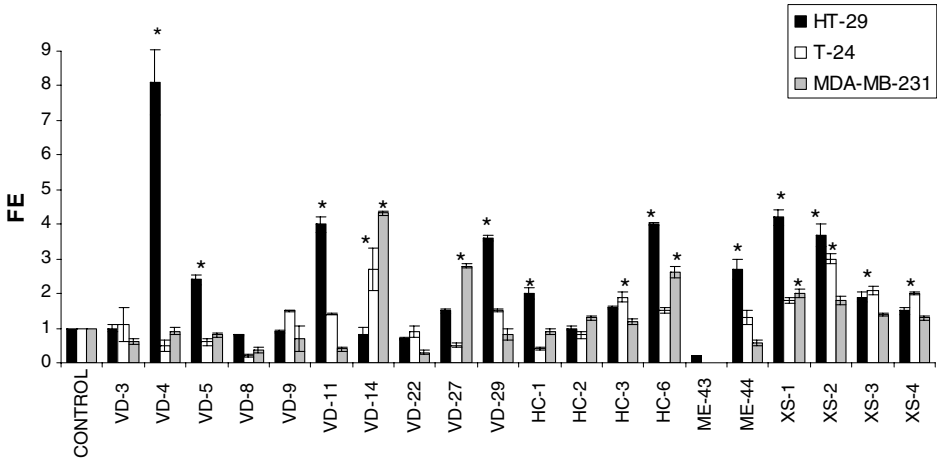

Figure 2. Determination of oligonucleosomal fragments in the cell lines of the study testing the compounds at IC_{50}. The figure represents the mean + SD of three different experiments comparing results with the respective control at each time of treatment (*$P < 0.05$).

cytometry in the case of HT-29 and T-24 cell lines. Because of the conglomerates that MDA-MB-231 cells form in suspension, the activation of caspase-3 was observed performing a substrate activation assay. The results of these assays are shown in Table 2.

2.3. Selectivity

In order to study the degree of selectivity, the cytotoxicity of the compounds was tested in cell cultures of two non-tumoral lines: CRL-8799 and CRL-11233, selected because they constitute an in vitro model often used for pharmacotoxicological studies.[24] Neutral red assay was chosen to test the cytotoxicity of the compounds in these cell lines. The highest IC_{50} value obtained from the tumoral cell lines for each compound was tested in this study. If the survival percentage is equal or higher than 85% the compound is considered non-cytotoxic (Fig. 3).

The best values were obtained with the compounds HC-1, HC-2, HC-6, XS-3, XS-4, ME17, and ME43.

HC-6, Bis-(4-methoxybenzyl)-pyrido[2,3-*d*]pyrimidine-2,4-diamine (Fig. 4), was selected due to its ability to induce apoptosis in the three tumoral cell lines tested, with good caspase-3 activator behavior being non-cytotoxic for the non-neoplastic cell lines. This compound showed the best activity among the selected compounds (Fig. 5A and B).

Table 2. Detection of activated caspase-3

		14 (h)	24 (h)	48 (h)
X-1	MDA-MB-231	–	+	–
	T-24	+	+	++
	HT-29	+	+	+
X-2	MDA-MB-231	–	–	–
	T-24	+	–	–
	HT-29	–	+	+
X-3	MDA-MB-231	–	–	–
	T-24	–	–	–
	HT-29	–	–	+
HC-1	MDA-MB-231	+	–	–
	T-24	+	+	++
	HT-29	–	–	–
HC2	MDA-MB-231	–	+	+
	T-24	–	+	+
	HT-29	–	–	+
HC-3	MDA-MB-231	–	–	+
	T-24	–	–	–
	HT-29	–	+	++
HC6	MDA-MB-231	–	–	–
	T-24	+	++	–
	HT-29	+	++	+
VD-3	MDA-MB-231	–	–	+
	T-24	–	–	–
	HT-29	–	–	–
VD11	MDA-MB-231	–	–	–
	T-24	–	–	–
	HT-29	–	–	+
ME-43	MDA-MB-231	–	–	+
ME-44	MDA-MB-231	–	–	–
	T-24	–	–	–
	HT-29	–	+	+

Results are expressed using the following symbols: (–) no increase of caspase-3 activation was detected comparing with the control. (+) the increase in activated caspase-3 is statistically significant ($p < 0.05$). (++) the increase in activated caspase-3 is statistically very significant ($p < 0.001$). Only data of active compounds are shown.

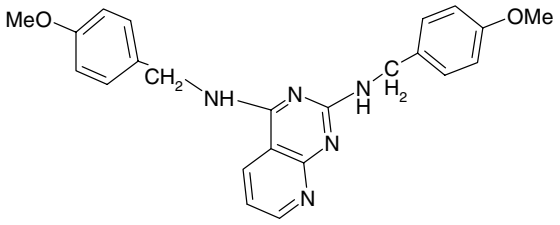

Figure 4. Chemical structure of the HC-6 compound.

2.4. Morphological changes induced by HC-6

Morphological changes induced by HC-6 were detected with 8 h of incubation. The apoptotic cells start to detach from the cultivation flask and an increase of cell death is observed as the time of incubation with HC-6 is extended (data not shown). These effects happened in the three cell lines studied.

2.5. Dose–response and time course effects of HC-6 on HT-29 and T-24 cells

HT-29 and T-24 cell lines were incubated with HC-6 for different periods of time at different concentrations and analyzed by flow cytometry. Incubation with a tenth of the IC_{50} (0,6 μM for T-24 and 0.89 μM for HT-29) during 24 h resulted in accumulation of cells in G2/M and a blockade of cell proliferation. About 50% and 40% of the HT-29 and T-24 cells, respectively, were arrested at G2/M with 4n content of DNA after 24-h incubation. This G2/M arrest is not associated either with morphological changes or with apoptosis (Fig. 6A). Treatment of HT-29 and T-24 cells with the IC_{50} values for each cell line resulted in a rapid appearance of cells with a DNA content less than G1, characteristic of apoptosis cells, with no previous changes in cell cycle. This induction of apoptosis is detectable after 8 h of incubation and progressively increased within 12 h of incubation (Fig. 6B).

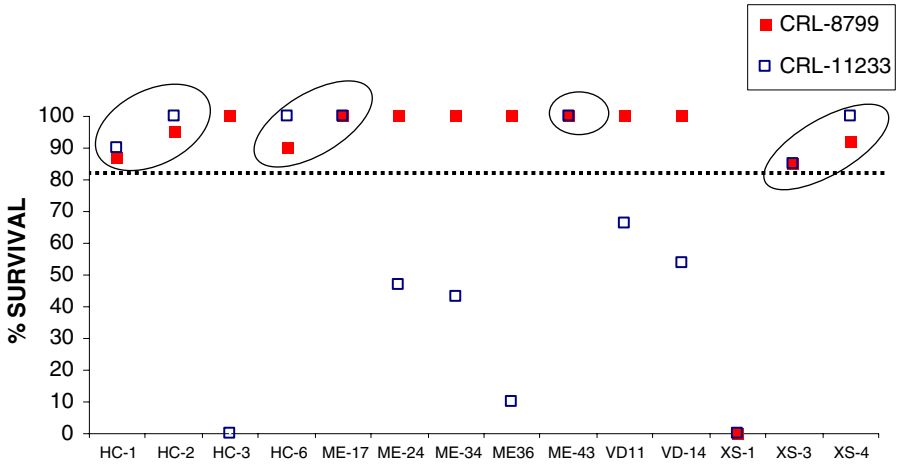

Figure 3. Survival percentage of treated CRL-8799 (■) and CRL-11233 (□) cell lines. Compounds that show no cytotoxic activity in these lines (survival ⩾ 85%) are surrounded by a circle.

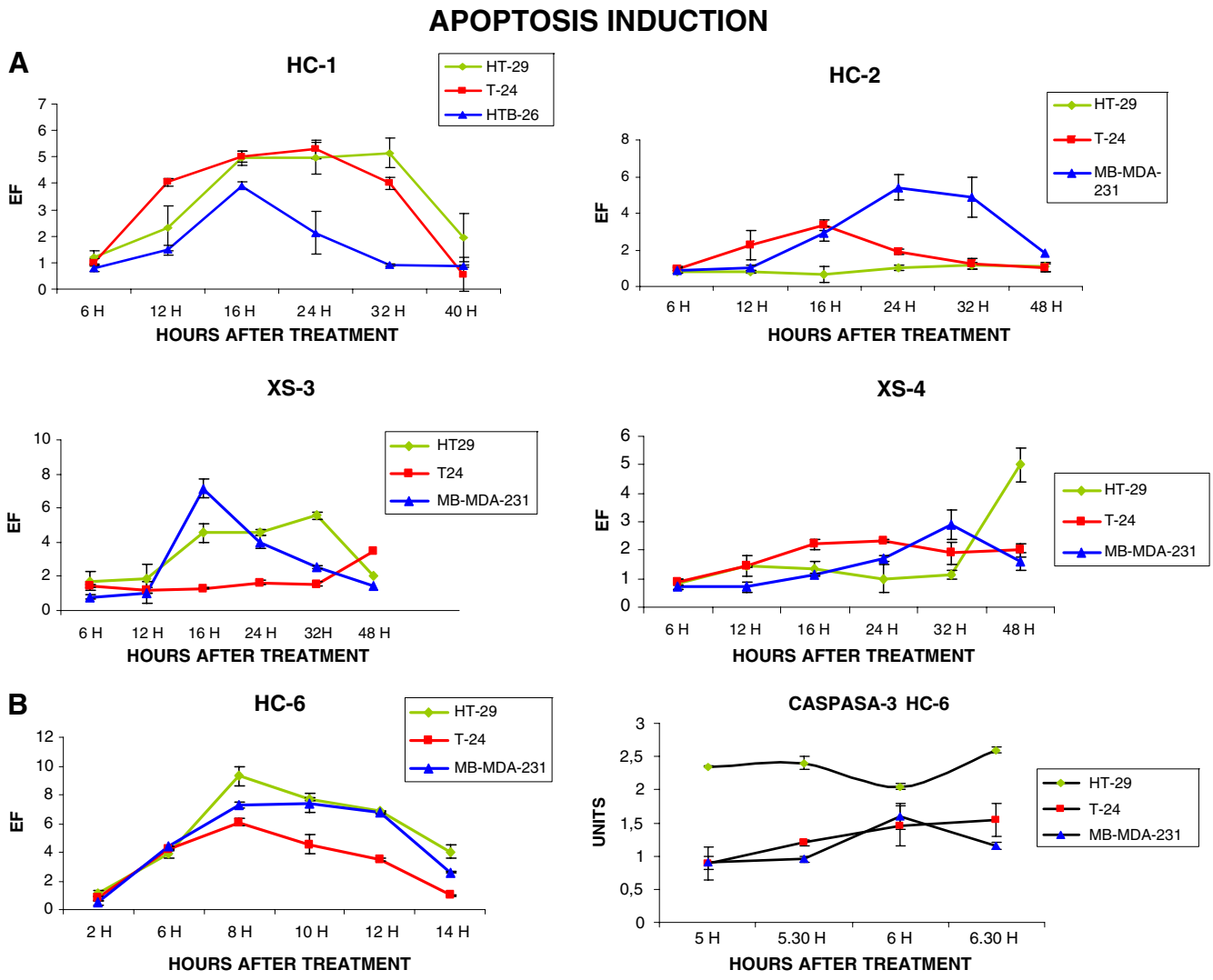

Figure 5. (A) Apoptotic effect of treatment with HC-1, HC-2, XS-3, and XS-4 in the three tumoral cell lines studied. (B) Effect of HC-6 as an apoptotic and caspase-3 activator.

2.6. Changes in gene expression induced by HC-6 during apoptosis

To elucidate the mechanism underlying the anticancer effect of HC-6, we investigated the effects of the compound in gene expression by using the microarray technology. HT-29 and T-24 cells were treated with their own IC_{50} value under conditions that induced caspase-3 activation (6 h) and DNA fragmentation (8 h) based on the results shown in Figure 5. Their gene expression patterns were compared with untreated control in the same slide. The experiment was performed in duplicate using the dye-swap technique. Tables 3 and 4 list the downregulated and upregulated genes.

Although, the relevance of some mRNAs that can be regulated by HC-6 treatment is not clear, we found significant changes in cell-cycle genes, apoptosis-related genes, and genes that coded DNA fragmentation proteins. DEAD (Asp-Glu-Ala-Asp) box polypeptide was downregulated with some other proteins related to DNA damage checkpoint mRNA (MDC1 protein). On the other hand, cyclin H and MAPKKK-13 have been found to be upregulated secondary to treatment with HC-6 in HT-29. Among the wide family of CEACAM, increased expression was observed in CEACAM-7 mRNA. In the same way, PAX8 gene was upregulated in colon cancer cell line (HT-29).

3. Conclusion

In the search of less toxic anticancer therapies we have looked for novel compounds with anticancer activity based on a proapoptotic mechanism. We synthesized novel symmetrical compounds based on bicyclic aromatic systems like pyrido[2,4-*d*]pyrimidines. The potential antitumoral activity of the compounds was evaluated in vitro and they were tested for cytotoxicity against three cancer cell lines; breast (MD-MBA-231), colon (HT-29), and urinary bladder (T-24). All the compounds showed anticancer activity against all the cell lines tested, with IC_{50} values in the micromolar range. The cytotoxic molecules were evaluated in apoptosis

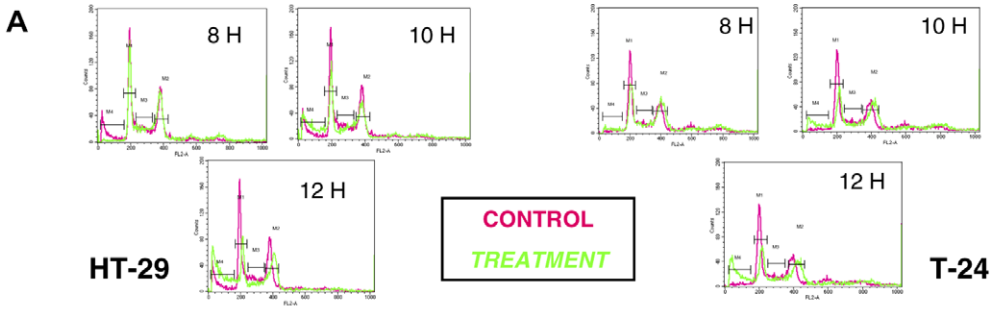

HT-29	G1	S	G2	SUB G1
CONTROL	51%	17%	30%	2%
8 H	35%	19%	38%	8%
10 H	22%	17%	36%	25%
12 H	17%	17%	33%	34%

T-24	G1	S	G2	SUB G1
CONTROL	48%	14%	33%	4%
8 H	36%	13%	43%	7%
10 H	28%	13%	40%	18%
12 H	26%	10%	36%	28%

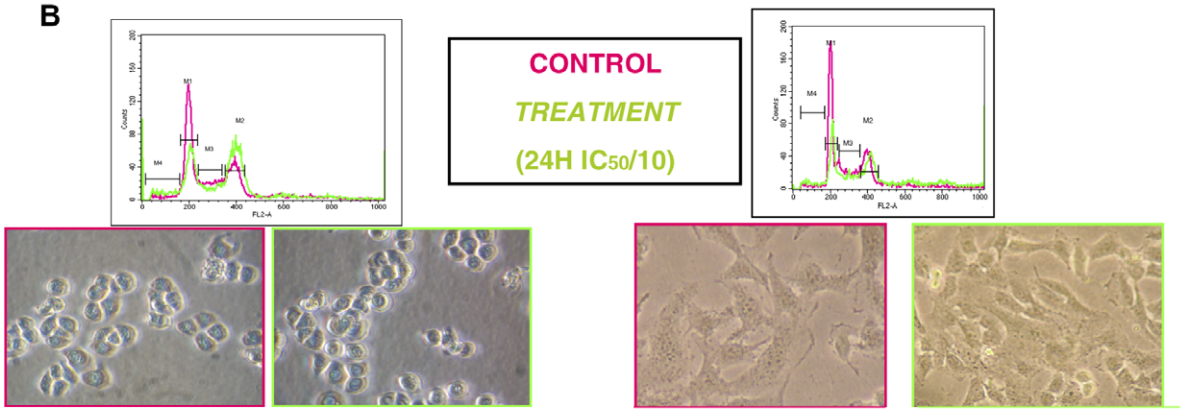

HT-29	G1	S	G2/M	SUB G1
CONTROL	49%	17%	29%	5%
24 H	30%	11%	52%	7%

T-24	G1	S	G2/M	SUB G1
CONTROL	55%	14%	26%	5%
24 H	42%	13%	38%	6%

Figure 6. Cells treated with IC_{50} (A) for 8, 10, and 12 h or $IC_{50}/10$ (B) for 24 h with HC-6. Control (pink) and treated cells (green) are shown in cell cycle diagrams and the percentages of distribution of cell cycle were reported. Data are representative of three different experiments.

assays and some of them exhibited great apoptosis induction, being able to promote caspase-3 activation and DNA fragmentation. The most promising compounds were tested against two non-tumoral cell lines (CRL-8799 and CRL-11233) and, among them, bis(4-methoxybenzyl)-pyrido[2,3-*d*]pyrimidine-2,4-diamine (HC-6) showed the best profile in these assays.

Our data also demonstrate that the apoptotic effect of HC-6 involves early caspase-3 activation and a subsequent DNA degradation within 10 h of incubation in all cell lines tested. In general, all compounds studied in this article have shown more apoptotic activity against the HT-29 cell line. Data reported here also demonstrate that MDA-MB-231 cells are less sensitive to this family of derivatives. The difference in sensitivity that cells show to cell death induced by HC-6 may be due to the diverse genomic aberrations typical of each cell line.

Furthermore, we found that HC-6 exerts two major dose- and time-dependent actions on cancer cells. At low concentrations mainly HC-6 affects the cell cycle without any effect on cell viability, and using higher concentrations, a transcription-independent apoptosis takes place. This ability of HC-6 has been previously described in other anticancer compounds like ET-743 (Yondelis, Trabectin).[25] The profile we have found secondary to HC-6 treatment seems to be very similar to the one that has been detected in several assays based on ET-743 treatment. This capacity can be explained on base of the different molecular pathways that are triggered depending on the dose.

To investigate the genes responsible for the induction of apoptosis, we carried out microarray analyses of the RNA expression profiles. These experiments were performed in order to determine the events involved in the induction of apoptosis. We found that the number

Table 3. Genes upregulated and downregulated in the HT-29 cell line exposed to the IC_{50} of HC-6 at two times

GenBank	Symbol	Description
Caspase-3 activation		
Upregulated		
NM_006890	CEACAM7	*Homo sapiens* carcinoembryonic antigen-related cell adhesion molecule 7
NM_003939	BTRC	*Homo sapiens* β-transducin repeat containing, transcript variant 2,
AF087970		*Homo sapiens* full length insert cDNA clone YU75B05
Downregulated		
AK021635		*Homo sapiens* ADNc FLJ11573, clone HEMBA1003376
DNA fragmentation		
Upregulated		
NM_013952	PAX8	*Homo sapiens* paired box gene 8, transcript variant PAX8C,
AL157447		*Homo sapiens* mRNA; cDNA DKFZp761C1811 (from clone DKFZp761C1811)
NM_004721	MAP3K13	*Homo sapiens* mitogen-activated protein kinase kinase kinase 13, mRNA
NM_001239	CCNH	*Homo sapiens* cyclin H
NM_000121	EPOR	*Homo sapiens* erythropoietin receptor
NM_005873	RGS19	*Homo sapiens* regulator of G-protein signaling 19
NM_000049	ASPA	*Homo sapiens* aspartoacylase (Canavan disease)
Downregulated		
AK024938		*Homo sapiens* ADNc: FLJ21285 fis, clone COL01912
AF056453		*Homo sapiens* clone TEE3
AF143326		*Homo sapiens* clone IMAGE:110578
AK021818		*Homo sapiens* cDNA FLJ11756 fis, clone HEMBA1005595
AK023612		*Homo sapiens* ADNc FLJ13550 fis, clone PLACE1007111
NM_004206	SEC22L3	*Homo sapiens* SEC22 vesicle trafficking protein-like 3 (*Saccharomyces cerevisiae*) transcript variant 2

of changes in gene expression induced by HC-6 was rather low. Apoptotic processes induced by radiation and some chemical compounds are shown to be transcription-independent, and in several studies made in p-53 null cells, few variations in gene expression have been observed while post-transcriptional changes seemed to be critical.[26,27] A similar behavior is shown in our work, and we considered that bis(4-methoxybenzyl)-pyrido[2,3-*d*]pyrimidine-2,4-diamine exerts its effects mainly through post-transcriptional changes, suggesting that cells have expressed the proper machinery needed to respond against HC-6 and start the apoptotic process. These results represent a working hypothesis that must be tested in future experiments.

According to the chemical structure, these compounds show high similarity with others which demonstrated tyrosine kinase inhibitory activity. Tyrosines have been broadly associated with different types of cancers and the overexpression/deregulation of this family of kinases may be of prognostic/predictive value in patients. Novel tyrosine kinase inhibitors are designed to exploit the molecular differences between tumor cells and normal tissues. At least 30 inhibitors are in various stages of clinical development in cancer (reviewed in).[28] Some of these small molecules possess well-defined clinical effects such as imatinib mesylate (STI571; Gleevec), gefitinib (Iressa), erlotinib (OSI-1774, Tarceva), lapatinib (GW-572016), canertinib (CI-1033), semaxinib (SU5416), vatalamib (CPTK787/7K222584), rorafenib (BAY443-9006), sutent (SU11248), and leflunomide (SU101). Some of them belong to the pyridopyrimidine family, as HC-6, and have demonstrated antitumoral properties against several cancer cells.[11,29–35]

In summary, our data indicate that HC-6 could be a very potent anticancer drug showing dose-dependent cytostatic and proapoptotic effects through activation of two different signaling pathways namely a pathway leading to cell cycle arrest and a transcription-independent route leading to rapid apoptosis.

4. Materials and methods

4.1. Cell lines and reagents

Five human cell lines were obtained from the American Tissue Culture Collection (Manassas, VA): HT29 (ATCC HTB 38), a colon adenocarcinoma cell line, T24 (ATCC HTB-24) from urinary bladder, MDA-MB-231 (ATCC HTB26) was established from adenocarcinoma of mammary gland, CRL8799 from breast epithelium (ATCC 184B5), and CRL11233 (ATCC THLE-3) from human liver.

HT29 and T24 cells were cultured in McCoys medium (Gibco), MDA-MB-231 in Leibovitz (Gibco), CRL8799 in MEG (Clonetics Corporation), and CRL11233 in BEGM (BEGM Bullet kit, Clonetics Corporation). These media were supplemented with 10% fetal bovine serum, penicillin (50 U/ml), and streptomycin (50 μg/mL). Cells were grown as monolayer in 175cc flasks (Corning) and were incubated at 37 °C in a humidified atmosphere containing 5% CO_2.

The evaluated compounds were dissolved in dimethylsulfoxide (DMSO). The DMSO concentration was

Table 4. Genes upregulated and downregulated in the MDA-MB-231 cell line exposed to the IC_{50} of HC-6 at two times

GenBank	Symbol	Description
Caspase-3 activation		
Upregulated		
NM_001900	CST5	*Homo sapiens* cystatin D
D50914		*Homo sapiens* mRNA for KIAA0124 gene, partial cds
Downregulated		
AB014576		*Homo sapiens* mRNA for KIAA0676 protein, partial cds
AF085847		*Homo sapiens* full length insert cDNA clone YI46G04
AF131760		*Homo sapiens* clone 24992 mRNA sequence, complete cds
AF131787		*Homo sapiens* clone 25248 mRNA sequence
AF254088		*Homo sapiens* EWS/ZSG fusion protein long B isoform (EWS/ZSG fusion) mRNA, complete cds
AJ278476		*Homo sapiens* partial mRNA for transport-secretion protein 2.2, (TTS-2.2 gene)
AK000090		*Homo sapiens* cDNA FLJ20083 fis, clone COL03440
AK001078		*Homo sapiens* cDNA FLJ10216 fis, clone HEMBA1006795
AK002177		*Homo sapiens* cDNA FLJ11315 fis, clone PLACE1010148
AK021879		*Homo sapiens* cDNA FLJ11817 fis, clone HEMBA1006421
AK023800		*Homo sapiens* cDNA FLJ13738 fis, clone PLACE3000194
AK024935		*Homo sapiens* cDNA: FLJ21282 fis, clone COL01907
AK026032		*Homo sapiens* cDNA: FLJ22379 fis, clone HRC07436
AL049445		*Homo sapiens* genomic DNA; cDNA DKFZp586A2322 (from clone DKFZp586A2322)
AL050088		*Homo sapiens* mRNA; cDNA DKFZp586B1817 (from clone DKFZp586B1817)
AL390083		*Homo sapiens* mRNA full length insert cDNA clone EUROIMAGE 363668
NM_000721	CACNAE1E	*Homo sapiens* calcium channel, voltage-dependent, alpha 1E subunit mRNA
NM_001618	PARP1	*Homo sapiens* poly(ADP-ribose) polymerase family, member 1
NM_001972	ELA2	*Homo sapiens* elastase 2, neutrophil mRNA
NM_002319	LRCH4	*Homo sapiens* leucine-rich repeats and calponin homology (CH) domain containing 4 mRNA
NM_002642	PIGC	*Homo sapiens* phosphatidylinositol glycan, class C transcript variant 2, mRNA
NM_003099	*SNX1*	*Homo sapiens* sorting nexin 1 transcript variant 1, mRNA
NM_004422	DVL2	*Homo sapiens* dishevelled, dsh homolog 2 (*Drosophila*) mRNA
NM_005447	PAMCI	*Homo sapiens* peptidylglycine alpha-amidating monooxygenase COOH-terminal interactor mRNA
NM_006007	ZA20D2	*Homo sapiens* zinc finger, A20 domain containing 2 mRNA
NM_006074	TRIM22	*Homo sapiens* tripartite motif-containing 22 mRNA
NM_006528	TFPI2	*Homo sapiens* tissue factor pathway inhibitor 2 mRNA
NM_006941	SOX10	*Homo sapiens* SRY (sex determining region Y)-box 10 mRNA
NM_013382	POMT2	*Homo sapiens* protein-*O*-mannosyltransferase 2 mRNA
Y10510		*Homo sapiens* mRNA for CD67S protein
DNA fragmentation		
Upregulated		
AL049361		*Homo sapiens* mARN; ADNc clone DKFZp566H243
AF086309		*Homo sapiens* full length insert cDNA clone ZD51E07
D50914		*Homo sapiens mRNA for KIAA0124 gene, partial cds*
Downregulated		
AF085847		*Homo sapiens* full length insert cDNA clone YI46G04
AF141347		*Homo sapiens* hum-a-tub2 alpha-tubulin mRNA, complete cds
AF210247	ENAM	*Homo sapiens* enamelin mRNA, partial cds
AF254088		*Homo sapiens* EWS/ZSG fusion protein long B isoform (EWS/ZSG fusion) mRNA, complete cds
AJ278476		*Homo sapiens* partial mRNA for transport-secretion protein 2.2, (TTS-2.2 gene)
AK000090		*Homo sapiens* cDNA FLJ20083 fis, clone COL03440
AK021879		*Homo sapiens* cDNA FLJ11817 fis, clone HEMBA1006421
AK023678		*Homo sapiens* cDNA FLJ13616 fis, clone PLACE1010916
AK023800		*Homo sapiens* cDNA FLJ13738 fis, clone PLACE3000194
AK026032		*Homo sapiens* cDNA: FLJ22379 fis, clone HRC07436
L34071		Human (clone SAA7C) mRNA sequence
NM_000899	KITLG	*Homo sapiens* KIT ligand transcript variant b, mRNA
NM_001972	*ELA2*	*Homo sapiens* elastase 2, neutrophil mRNA
NM_002319	LRCH4	*Homo sapiens* leucine-rich repeats and calponin homology (CH) domain containing 4 mRNA
NM_003099	SNX1	*Homo sapiens* sorting nexin 1 transcript variant 1, mRNA
NM_003323	TULP2	*Homo sapiens* tubby like protein 2 mRNA
NM_004396	DDX5	*Homo sapiens* DEAD (Asp-Glu-Ala-Asp) box polypeptide 5 mRNA
NM_006403	NEDD9	*Homo sapiens* neural precursor cell expressed, developmentally down-regulated 9 transcript variant 1, mRNA
NM_006528	TFPI2	*Homo sapiens* tissue factor pathway inhibitor 2 mRNA
NM_006941	SOX10	*Homo sapiens* SRY (sex determining region Y)-box 10 mRNA
NM_014641	MDC1	*Homo sapiens* mediator of DNA damage checkpoint 1 mRNA
NM_016124		*Homo sapiens* Rhesus blood group, D antigen (RHD), transcript variant 1, mRNA
NM_016131	RAB10	*Homo sapiens* RAB10, member RAS oncogene family mRNA

equalized in all media. In all cases, the concentration of solvent in culture medium did not exceed 0.5% (v/v).

4.2. Cytotoxicity study

Cytotoxicity was determined by using the neutral red assay as described by Lowik et Albas.[36] Ninety-six-well flat-bottomed tissue culture plates (Microtest 96 Falcon, Becton–Dickinson) were used for the experiments. Briefly, 20,000 cells were resuspended in each well and incubated overnight to assess their attachment. The tested compounds or vehicle was added and incubated for 72 h. The cells were washed with PBS and incubated for 2 h with a neutral red solution. The dye was extracted adding NaH_2PO_4 in 50% ethanol. The absorbance was measured at 540 nm using 650 nm as a reference wavenlength with a microtiter plate reader (Organon Teknica).

The screening concentrations of the compounds were 20 and 100 μM. The results were expressed as the average of three different experiments. The IC_{50} values were calculated for each compound using a range of, at least, six concentrations. The IC_{50} value was determined using a curvilinear regression model with the statistical software SPSS 11.0.

With regard to selectivity, cytotoxicity was determined in cell cultures of two non-tumoral lines, CRL-7899 and CRL-11233. The highest IC_{50} calculated in the three tumoral lines was selected as the test concentration for assays on non-tumoral cells. The IC_{50} obtained in MDA-MB-231 was evaluated in breast non-tumoral cells.

4.3. DNA fragmentation analysis

The presence of soluble histone–DNA complexes was measured by using the Cell Death Detection ELISA Plus kit (Roche). For this assay cells were seeded on 96-well plates at a density of 20,000 cells/well and incubated with the compounds for 24 or 48 h. Cell Death ELISAs were performed according to the manufacturer's instructions. Specific enrichment of mono- and oligonucleosomes released into the cytoplasm (enrichment factor, EF) was calculated as the ratio between the absorbance values of the samples obtained from treated and control cells.

4.4. Measurement of caspase-3 activity by cytometry

Detection of active caspase-3 was carried out by means of cytometry, using the Active-Caspase-3 FITC Mab apoptosis kit (Pharmingen), which evaluates the number of cells that contain the dimerized and activated form of caspase-3, according to manufacturer. The range of effective measurements for this enzyme was found to be between 14 and 48 h. Therefore, measurements were taken at 14, 24, and 48 h, and the obtained values were compared with the control cells incubated without the test compounds. The tested concentrations correspond to the IC_{50} values determined in the cytotoxicity assay. Cytometry was performed on a FACSCAN (Becton–Dickinson).

4.5. Measurements of caspase-3 activity by a substrate assay

Caspase-3 assays were carried out in plates of 9 cm diameter (Cellstar Greiner Bio-one). Cells were harvested by using a 0.25% trypsin/0.03 EDTA solution and then lysed with a buffer containing 1% Triton (100×); 50 mM Tris–HCl, pH 8; 150 mM NaCl, 100 μg/mL PMSF; 1 mM DTT. The soluble fraction of the cell lysate was then assayed for caspase-3 activity using Ac-DEVD-pNA, a colorimetric substrate for caspase-3. 80 μg of protein was diluted in 50 μL of caspase-3 buffer containing 50 mM HEPES, pH 7.4, 100 mM NaCl, 0.1% CHAPS, 10 mM DTT, 1 mM EDTA, and 10% glycerol. Fifty microliters of the substrate, DEVD-pNa (Biomol), was added to a final concentration of 200 μM, and the plates were incubated for 24 h at 37 °C and 5% CO_2. Levels of released *p*-nitroanitrile (pNA) were measured as absorbance at 405 nm. To confirm the correlation between caspase-3 activity and signal detection, control reactions were performed by addition of 1 μL of 1 mM DEVD-CHO (Biomol), an inhibitor of caspase-3 to the diluted protein samples followed by addition of the reaction buffer and incubation at 37 °C for 30 min before adding the caspase-3 substrate.[37–39]

4.6. Cell cycle analysis

Single cell suspensions were obtained from cell monolayers as follows. First, cells were washed with PBS and then incubated for 5 min with trypsin. Cells were collected from the dishes in the presence of PBS and were washed and resuspended in 1 mL of PBS. For cell cycle analysis, cells were fixed with ice-cold 100% ethanol and incubated at 4 °C for 15 min. Cells were then resuspended in 125 μL of ribonuclease type IIA and incubated at 37 °C for 15 min, then resuspended in 125 μL of propidium iodine (25 μg/mL) and incubated at room temperature for 30 min in the dark. Before DNA content analysis cells were filtered by 40 μm nylon mesh filter. The analysis was performed on a Becton–Dickinson FACScan flow cytometer using the CellQuest Software. All the results were obtained from three independent experiments.

4.7. cDNA microarray

The different cell lines were seeded at a rate of 8×10^6 cells per flask during 14 h and then were treated with DMSO (vehicle control) or IC_{50} of HC-6 for two different times (caspase-3 activation and DNA fragmentation). The rationale for choosing these time points was to capture gene expression profile of early response genes, and those involved in the induction of apoptosis.

Total RNA from each sample was isolated using the RNeasy Midi Kit and RNAse-free DNAse Set (Qiagen, Valencia, CA) according to the manufacturer's protocols. The RNA concentration was calculated by

spectrophotometry and it was adjusted to 1 μg/μL. Quality control of RNA integrity was performed by electrophoresis on a 2% agarose gel using ethidium bromide staining.

The 3DNA Submicro Oligo Expression Detection Kit (Genisphere) was used to perform reverse transcription as recommended by manufacturer; afterward, cDNA was prehybridized with the fluorescent reactive 3DNA. Then, the samples were hybridized to the slides from the Cent for Applied Genomics of the University of NewJersey. These slides contain 18.861 oligos. After overnight hybridization at 50 °C in a slide cassette (Telechem, Sunnyvale, CA), slides were washed sequentially in a series of solutions with increasing stringency: 2× SSC, 0.2% SDS during 5 min at room temperature; 2× SSC 0.2% SDS, 15 min, 42 °C; 2× SSC, during 10 min at room temperature; and finally 0.2× SSC during 10 min at room temperature.

To remove the systematic bias caused by the chemical difference between Cy3 and Cy5, each microarray study was performed twice using dye-swap.

4.8. Microarray data acquisition, normalization, and analysis

The hybridized slides were scanned with the GMS 418 scanner (Genetic Microsystems, Woburn, MA). After image acquisition, the scanned images were imported into 'ImaGene 4.1' software (BioDiscovery) to quantify the signal intensities. Data from spots not recognized by the Imagene analysis software were excluded from further considerations (empty, poor, and negative spots). We also removed data from spots identified as visually flawed. The fluorescent median signal intensity for each spot was calculated using local median background subtraction. Data were normalized using Global mean, Dye-swap Pairs normalization, and Dye Swap Fix filter 1.5 with the program ArrayNorm 1.7 software (Graz, Austria).[40] Log ratios above 2 or below -2 were considered as differential expression.

4.9. Statistics

Data are presented as means ± SD. IC_{50} values were analyzed using a non-linear regression model. Non-parametric or parametric tests were performed according to the normality test results. The SPSS 11.0 software was used for all statistical analyses.

Acknowledgments

The authors wish to express their gratitude to the University of Navarra Research Plan (*Plan de Investigación de la Universidad de Navarra, PIUNA*) for its financial support to the project. Lucia Cordeu was supported by a pre-doctoral fellowship from *Gobierno de Navarra*. We thank the Center for Applied Genomics and the New Jersey Commision on Science and Technology for providing the Oligo 19K human Array.

Supplementary data

Supplementary data associated with this article can be found, in the online version, at doi:10.1016/j.bmc.2006.12.010.

References and notes

1. Fesik, S. W. *Nat. Rev. Cancer* **2005**, *5*, 876.
2. Bold, R. J.; Termuhlen, P. M.; McConkey, D. J. *Surg. Oncol.* **1997**, *6*, 133.
3. Reed, J. C. *Curr. Opin. Oncol.* **1999**, *11*, 68.
4. Reed, J. C. *Am. J. Pathol.* **2000**, *157*, 1415.
5. Degterev, A.; Boyce, M.; Yuan, J. *Oncogene* **2003**, *22*, 8543.
6. Cohen, G. M. *Biochem. J.* **1997**, *326*(Pt. 1), 1.
7. Budihardjo, I.; Oliver, H.; Lutter, M.; Luo, X.; Wang, X. *Annu. Rev. Cell Dev. Biol.* **1999**, *15*, 269.
8. Brown, J. M.; Attardi, L. D. *Nat. Rev. Cancer* **2005**, *5*, 231.
9. Mita, M.; Tolcher, A. W. *Curr. Probl. Cancer* **2005**, *29*, 8.
10. Galmarini, C. M.; Jordheim, L.; Dumontet, C. *Expert. Rev. Anticancer Ther.* **2003**, *3*, 717.
11. Zhou, Y.; Li, S.; Hu, Y. P.; Wang, J.; Hauser, J.; Conway, A. N.; Vinci, M. A.; Humphrey, L.; Zborowska, E.; Willson, J. K.; Brattain, M. G. *Cancer Res.* **2006**, *66*, 404.
12. Wisniewski, D.; Lambek, C. L.; Liu, C.; Strife, A.; Veach, D. R.; Nagar, B.; Young, M. A.; Schindler, T.; Bornmann, W. G.; Bertino, J. R.; Kuriyan, J.; Clarkson, B. *Cancer Res.* **2002**, *62*, 4244.
13. Wissing, J.; Godl, K.; Brehmer, D.; Blencke, S.; Weber, M.; Habenberger, P.; Stein-Gerlach, M.; Missio, A.; Cotten, M.; Muller, S.; Daub, H. *Mol. Cell Proteom.* **2004**, *3*, 1181.
14. Guo, X. N.; Zhong, L.; Tan, J. Z.; Li, J.; Luo, X. M.; Jiang, H. L.; Nan, F. J.; Lin, L. P.; Zhang, X. W.; Ding, J. *Cancer Biol. Ther.* **2005**, *4*, 1125.
15. Cockerill, S.; Stubberfield, C.; Stables, J.; Carter, M.; Guntrip, S.; Smith, K.; McKeown, S.; Shaw, R.; Topley, P.; Thomsen, L.; Affleck, K.; Jowett, A.; Hayes, D.; Willson, M.; Woollard, P.; Spalding, D. *Bioorg. Med. Chem. Lett.* **2001**, *11*, 1401.
16. Dorsey, J. F.; Jove, R.; Kraker, A. J.; Wu, J. *Cancer Res.* **2000**, *60*, 3127.
17. Levitzki, A. *Eur. J. Cancer* **2002**, *38*(Suppl. 5), S11.
18. Vlahovic, G.; Crawford, J. *Oncologist* **2003**, *8*, 531.
19. Krause, D. S.; Van Etten, R. A. *N. Eng. J. Med.* **2005**, *353*, 172.
20. Cubedo, E.; Cordeu, L.; Bandres, E.; Rebollo, A.; Malumbres, R.; Sanmartin, C.; Font, M.; Palop, J. A.; Gacia-Foncillas, J. *Cancer Biol. Ther.* **2006**, *5*, 850.
21. Echeverria, M.; Mendivil, B.; Cordeu, L.; Cubedo, E.; Garcia-Foncillas, J.; Font, M.; Sanmartin, C.; Palop, J. A. *Arch. Pharm. (Weinheim)* **2006**, *339*, 182.
22. Font, M.; Ardaiz, E.; Cordeu, L.; Cubedo, E.; Garcia-Foncillas, J.; Sanmartin, C.; Palop, J. A. *Bioorg. Med. Chem.* **2006**, *14*, 1942.
23. Sanmartin, C.; Echeverria, M.; Mendivil, B.; Cordeu, L.; Cubedo, E.; Garcia-Foncillas, J.; Font, M.; Palop, J. A. *Bioorg. Med. Chem.* **2005**, *13*, 2031.
24. Pfeifer, A. M.; Cole, K. E.; Smoot, D. T.; Weston, A.; Groopman, J. D.; Shields, P. G.; Vignaud, J. M.; Juillerat, M.; Lipsky, M. M.; Trump, B. F., et al. *Proc. Natl. Acad. Sci. U.S.A.* **1993**, *90*, 5123.
25. Gajate, C.; An, F.; Mollinedo, F. *J. Biol. Chem.* **2002**, *277*, 41580.
26. Ofir, R.; Zhang, L. C.; Kyne, A. P.; Houtzager, V.; O'Connor, L.; Adams, J. M. *DNA Cell Biol.* **2000**, *19*, 29.

27. Nister, M.; Tang, M.; Zhang, X. Q.; Yin, C.; Beeche, M.; Hu, X.; Enblad, G.; van Dyke, T.; Wahl, G. M. *Oncogene* **2005**, *24*, 3563.
28. Madhusudan, S.; Ganesan, T. S. *Clin. Biochem.* **2004**, *37*, 618.
29. Wolff, N. C.; Veach, D. R.; Tong, W. P.; Bornmann, W. G.; Clarkson, B.; Ilaria, R. L., Jr. *Blood* **2005**, *105*, 3995.
30. Mizenina, O. A.; Moasser, M. M. *Cell Cycle* **2004**, *3*, 796.
31. Huron, D. R.; Gorre, M. E.; Kraker, A. J.; Sawyers, C. L.; Rosen, N.; Moasser, M. M. *Clin. Cancer Res.* **2003**, *9*, 1267.
32. Raymond, E.; Faivre, S.; Armand, J. P. *Drugs* **2000**, *60*(Suppl. 1), 15.
33. Bridges, A. J. *Curr. Med. Chem.* **1999**, *6*, 825.
34. Rewcastle, G. W.; Bridges, A. J.; Fry, D. W.; Rubin, J. R.; Denny, W. A. *J. Med. Chem.* **1997**, *40*, 1820.
35. Barvian, M.; Boschelli, D. H.; Cossrow, J.; Dobrusin, E.; Fattaey, A.; Fritsch, A.; Fry, D.; Harvey, P.; Keller, P.; Garrett, M.; La, F.; Leopold, W.; McNamara, D.; Quin, M.; Trumpp-Kallmeyer, S.; Toogood, P.; Wu, Z.; Zhang, E. *J. Med. Chem.* **2000**, *43*, 4606.
36. Lowik, C. W.; Alblas, M. J.; van de Ruit, M.; Papapoulos, S. E.; van der Pluijm, G. *Anal. Biochem.* **1993**, *213*, 426.
37. Darmon, A. J.; Nicholson, D. W.; Bleackley, R. C. *Nature* **1995**, *377*, 446.
38. Lazebnik, Y. A.; Kaufmann, S. H.; Desnoyers, S.; Poirier, G. G.; Earnshaw, W. C. *Nature* **1994**, *371*, 346.
39. Datta, R.; Kojima, H.; Yoshida, K.; Kufe, D. *J. Biol. Chem.* **1997**, *272*, 20317.
40. Pieler, R.; Sanchez-Cabo, F.; Hackl, H.; Thallinger, G. G.; Trajanoski, Z. *Bioinformatics* **2004**, *20*, 1971.